



Accuracy of tree geometric parameters depending on the LiDAR data density

Edyta Hadaś^{1*} and Javier Estornell²

¹Institute of Geodesy and Geoinformatics, Wrocław University of Environmental and Life Sciences,
Grunwaldzka 53, 50-357, Wrocław, Poland

²Geo-Environmental Cartography and Remote Sensing Group (CGAT),
Department of Cartographic Engineering, Geodesy and Photogrammetry,
Universitat Politècnica de València, Camino de Vera s/n, 46022, Valencia, España

*Corresponding author, e-mail address: edyta.hadas@up.wroc.pl

Abstract

The aim of this study was to compare geometric parameters of olive trees (tree height, crown base height, crown diameters, crown area), using LiDAR data of different densities: 0.5, 3.5 and 9 points m⁻². Two strategies were proposed and verified with a focus on raster and raw data analysis. Statistical tests have shown, that for the tree height and crown base height estimation, the choice of strategy was irrelevant, but denser LiDAR data provided more accurate results. The raster analysis strategy applied for sparse and dense LiDAR datasets allowed crown shape to be determined with a similar accuracy which means raster data are useful for estimating other indirect tree parameters. The quality of results was independent from the tree size.

Keywords: Remote sensing, dendrometry, LiDAR, agriculture.

Introduction

Tree height, crown base height and crown diameter constitute very important tree geometric parameters for the management and planning of agricultural production. The reliable knowledge of these parameters allows growth to be predicted, to plan pruning, fertilizer inputs, irrigation requirements or pesticide dose [Doruska and Burkhart, 1994; Brunner, 1998], which directly affect the efficiency of cultivation. However, manual methods of obtaining tree geometric parameters are very time-consuming. For this reason, automatic methods of acquiring dendrometric characteristics over large areas have been under development for more than a decade.

Formerly, optical remote sensing techniques and microwave satellite imaging were used to acquire data for the inventory [Tomppo, 1997]. Significant developments in airborne laser scanning allowed the use of remote sensing techniques for tree inventory purposes, as well. Light Detection and Ranging (LiDAR) is an active sensor, which emits a series of laser pulses toward measured objects. In airborne laser scanning, the sensor is located on a flying

platform and directed toward the ground. The time difference between pulse emission and reception of the reflected pulse is converted into the distance between the sensor and the measured point [Lefsky et al., 2002; Evans et al., 2009]. Currently, LiDAR data are typically characterised by a much better accuracy than passive, optical or satellite data. A single LiDAR pulse can be reflected more than once [Evans et al., 2009]. In forest areas, the first reflection usually originates from the top of tree canopy and the last one originates from the ground surface. Proper filtering and processing of LiDAR data allows for a determination of Digital Terrain Model (DTM) and Canopy Height Model (CHM) [Ramdani, 2013]. Moreover, the intermediate pulses can be used to determine the characteristics of the tree canopy. Precise measurements of the geometric parameters of individual trees over a large area have been feasible since late '90 [Brandtberg, 1999; Hyyppä and Inkinen, 1999], which is particularly important from both economical and time-saving points of view [St-Onge et al., 2003; Reutebuch et al., 2005].

The vast majority of research in the field of remote sensing of tree geometric parameters is devoted to the forest inventory. LiDAR data are commonly used for the estimation of tree heights [Morsdorf et al., 2004; Yu et al., 2004; Andersen et al., 2006; Hopkinson et al., 2007; Edson and Wing, 2011; Saremi et al., 2014], crown base heights [Vauhkonen, 2010], crown dimensions [Means et al., 2000; Popescu and Zhao, 2008], crown volume [Hinsley et al., 2002; Riaño et al., 2004], stem diameter [Popescu, 2007; Saremi et al., 2014], stem volume [Persson et al., 2002; Straub and Koch, 2011], and leaf area index [Roberts et al., 2005; Pope and Treitz, 2013; Sabol et al., 2014]. These parameters can be used for the indirect estimation of the biomass volume [Hauglin et al., 2013; Kankare et al., 2013], in order to avoid destructive methods for direct biomass volume measurement by cutting and weighing the pieces of wood [Araújo et al., 1999; Velázquez-Martí et al., 2010]. The most common approach of biomass volume measurement is regression modeling, based on the diameter of breast height (DBH) and tree height [Araújo et al., 1999; Francis, 2000]. Reliable estimation of the biomass of forest ecosystems is a very important climatological issue, as it can be combined with estimates of the vegetation productivity for the assessment of the magnitude and rate of carbon sequestration, autotrophic respiration, in addition to the amount of carbon emitted to the atmosphere when the ecosystem is disturbed [Houghton et al., 2009].

In the biomass estimation for forest areas, the stem characteristics are the most important indicators, since the substantial proportion of the woody biomass is concentrated in the stem. In the case of agricultural trees, the stem is usually short and the main part of biomass is concentrated in the crown [Velázquez-Martí et al., 2014]. Therefore, for agricultural purposes, the characteristics of crown-related parameters are of crucial interest. Moreover, crown parameters of agricultural trees are related to the main function of those trees, which are used in the fruit production. Large and branchy crowns have a positive influence on the protection and remediation of soil, reducing the impact of rain and other factors causing soil erosion [Rodríguez et al., 2008]. In this context, the knowledge of crown geometric parameters of agricultural trees allows more efficient management of agricultural production, a prediction of the vegetation growth and a forecast of the harvest.

Precise remote estimation of tree geometric parameters, and subsequent biomass estimation, require a high density of LiDAR data. If only sparse LiDAR data is available, these should be

supported with an additional data source, e.g., with high-resolution optical imagery [Sheridan et al., 2015]. This is especially important for dense vegetation, as one of the demanding tasks is to extract the geometry of an individual tree. When agricultural trees are subject to remote measurements, the extraction of the geometry can be achieved easily, because the trees are usually isolated from each other. A case study for determining wood volume and height of olive trees using LiDAR data on the basis of plots without extracting and delineating individual tree parameters, can be found in Estornell et al. [2014]. There is a growing availability of LiDAR data which cover large areas and have various characteristics. LiDAR data of low density are already available in some countries. For example, in Spain, LiDAR data are collected every 6 years, because arboriculture is an important branch of farming there. Therefore, it is advisable to study the potential of LiDAR data for the parameter estimation of individual trees which has not been studied yet. In forestry analyses, low density LiDAR data may be insufficient for the prediction of individual tree parameters according to the previous studies in forest environments [Hyypä and Inkinen, 1999; Holmgren and Persson, 2003; Magnussen et al., 1999]. However, a further analysis is required to investigate whether low density LiDAR data can be used for estimating structure parameters of fruit trees in agricultural environments, wherein the trees are typically isolated, which may be beneficial particularly in the Mediterranean zone. This was the main motivation to perform the study presented in this paper.

The aim of this study was to analyse the accuracy of automatically-determined geometric parameters of trees depending on the density of LiDAR data. Consequently, the objective of this research was to investigate whether the low density LiDAR data can be used for a reliable estimation of tree height, crown base height, average crown diameter, and crown area. It was also investigated, whether the accuracy of estimated tree geometric parameters depends on the tree size and whether the results depend on the estimation strategy.

Data and methodology

Study area

The study area is located in the West Central part of Spain, in the Castellon province, Viver district, about 70 km northeast from city of Valencia. The study area of 5.92 ha constitutes a rectangular plot defined by UTM coordinates: $X_{max} = 4420725$, $Y_{max} = 704365$, $X_{min} = 4420360$, $Y_{min} = 704210$, zone 30 N, in the European Terrestrial Reference System 1989. Olive trees (*Olea europea L.*) have been cultivated for many years in this particular area.

LiDAR data and orthophotomap

Two sets of discrete LiDAR point clouds, acquired during two independent campaigns, are available for the study area. The point coordinates in both datasets are expressed in the European Terrestrial 1989 (ETRS89) reference system, UTM projection, zone 30. The structure of trees remained unchanged between two measurement campaigns, because trees were pruned in two phases every year. First, a mechanical pruning was performed by topping; afterwards, 50% shoots and damaged branches were removed in the inner crown through manual cutting with shears. This second pruning was aimed at providing lighted and aired conditions to the crowns in order to stabilize production. Therefore, the height

from the base of a tree to the top did not change between the both LiDAR campaigns.

The first dataset (referred hereinafter as the sparse one) was collected in November 2009. It comes from the publicly accessible LiDAR dataset which covers the entire area of Spain. Data were downloaded from the Institut Cartogràfic Valencià of the Valencia region (<http://centrodedescargas.cnig.es/CentroDescargas/>). The LiDAR data were acquired using a Leica ALS60 sensor with the following parameters: average flight height of 3070 m above the sea level, pulse frequency of 93.9 kHz, scan frequency of 33.7 Hz, field of view (FOV) 50°, flight speed 70 ms⁻¹ and the nominal pulse density of 0.5 points m⁻².

The second dataset (referred hereinafter as a dense one) was acquired in September 2012 using a Leica ALS50-II laser scanner with the average flight height of 1500 m (AGL), pulse frequency of 150 kHz; scan frequency of 88 Hz; field of view (FOV) 18°, nominal pulse density of 4 points m⁻², the density, however, was not uniform over the entire area. One part of the study area covered by overlaying scans has an average density of 9 points m⁻², whereas the remaining area has an average density of 3.5 points m⁻².

During the field measurements, 62 points located near the trees were measured with GPS Real Time Kinematic (RTK) technique using the Leica System 1200 receiver. This measurement campaign was undertaken in order to verify the quality of the digital terrain model which was subsequently obtained from LiDAR data.

Finally, an orthophoto in near-infrared spectrum was available with a nominal resolution of 0.5 m from ©Institut Cartogràfic Valencià of the Valencia region (Spain). This orthophoto provided reference information on approximated crown tree centres. Although the accuracy of centroids was limited by the resolution of the image, the orthophoto can be considered as a good approximation for a comparison between the orthophoto-derived crown centroids and those obtained from LiDAR data.

Field measurements

25 samples of individual trees were selected and numbered from 1 to 25, 13 trees (no. 1-13) were inside the area of overlaying scans (see Fig. 1). For 25 selected trees, the following parameters were measured using traditional dendrology methods: tree height, crown base height (also defined in the literature as stem height), stem diameter, length of the longest crown diameter and length of a crown diameter perpendicular to the longest one. Traditional equipment commonly exploited in forestry was used for the measurements: a diameter tape and a metric pole. The lengths of two perpendicular diameters were used to determine the average crown diameter. The measurement of stem diameter was used to classify the trees into two groups, according to the size of tree. A tree was considered as medium, when its stem diameter was smaller than 25 cm, and considered as large, when its stem diameter was larger than 40 cm. It is important to note here that none of the 25 selected trees had the stem diameter between 25 cm and 40 cm, which implies that the proposed division was very natural. Basic statistics of measured tree parameters for selected trees are presented in Table 1.

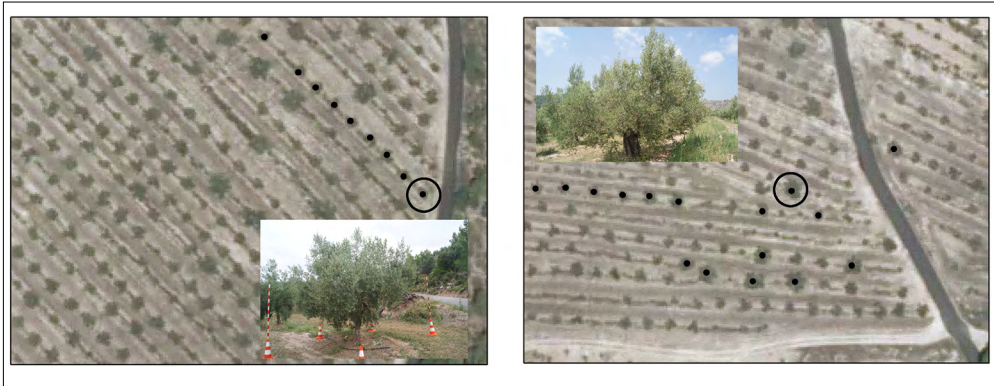


Figure 1 - Orthophotomap of parts of study area including 25 samples of individual trees.

Table 1 - Basic statistics of measured tree parameters.

	Tree height (m)			Crown base height (m)			Average crown diameter (m)		
	all trees	medium trees	large trees	all trees	medium trees	large trees	all trees	medium trees	large trees
Average	3.73	3.63	3.95	0.82	0.77	0.93	4.01	3.50	5.08
Std. dev.	0.32	0.27	0.31	0.13	0.07	0.15	0.86	0.32	0.65
Maximum	4.48	4.23	4.48	1.07	0.88	1.07	6.38	4.12	6.38
Minimum	3.12	3.12	3.49	0.60	0.62	0.60	3.04	3.04	4.07

Digital Terrain Model, Canopy Height Model and crown centers

Generating a Digital Terrain Model (DTM) was the first step of processing LiDAR data. Several different approaches and two different pieces of software were used for this purpose: ArcGIS® software by Esri and FUSION (Silviculture and Forest Models Team of the US Forest Service, Seattle, WA, USA). In the FUSION software, different numbers of iterations were used (3 and 8) for filtering out ground points from the original point cloud, and then DTM grids were generated using different cell sizes for intermediate surface models (see manual of fusion command groundfilter http://forsys.cfr.washington.edu/fusion/FUSION_manual.pdf) : 1x1 m, 2x2 m, 4x4 m, 5x5 m and 10x10 m. The latter three cell sizes were used for the both sparse and dense datasets, but the first two cell sizes were used only for the dense dataset. The density of 0.5 points m⁻² appeared to be insufficient to obtain redundant information inside such small cell sizes, and thus, the data filtering failed. In the ArcGIS software the same cell sizes were also used. Two approaches providing cell heights were investigated: first using the average height and the second one using the minimum height of points inside a cell. The quality of obtained DTMs was evaluated by calculating a mean bias and a standard deviation of height residuals between the DTM and GPS-RTK measured points.

After generating DTMs, the point clouds were normalised, in order to determine relative heights of LiDAR points with respect to DTMs. This step was necessary for a proper extraction of the tree heights and tree crown base heights, which were measured from the

ground directly below the tree. From both normalised datasets, the CHM were created as continuous grid surfaces representing relative heights of trees with the maximum available resolution. The grid size of each CHM had been chosen to fit the density of respective dataset, therefore, the 0.5x0.5 m CHM was created for the dense dataset and the 1x1 m CHM was created for the sparse dataset.

Having a CHM, it was possible to automatically determine the approximated location of each tree by slicing a CHM raster. A raster slicing is a method of raster classification, with user-defined data ranges (slice heights). The results of raster slicing may be provided as a polygons, defining the boundaries between classes. When only one single slice height is defined for CHM, we can consider the resulting polygons as approximated crown areas, and a tree center may be obtained as a centroid of each polygon. This is a fully automatic method, wherein the slice height is the only parameter that should be defined. In this study, we decided to search for the optimal height slice which would provide the most accurate tree centers. The CHM models obtained from the sparse and dense dataset were thus sliced using ENVI software (Exelis Visual Information Solutions, Boulder, Colorado) at heights from 0.0 m to 5.0 m with an interval of 0.1 m. For each slice height the tree centroids were automatically obtained, and for each centroid the distance to the centroid derived from orthophoto was calculated. The optimal slice height was chosen as the one where the standard deviation of distances was the smallest.

Crown shape and area

A subset of LiDAR points was selected belonging to the individual tree and, eventually, to the tree's close surroundings in order to determine the tree height, crown base height, and crown diameters. Two different strategies were applied at this point: A - using polygons derived from slicing a CHM raster at the height of 0.5 m, B - using the circular buffer zone around the tree centroid. The strategies are referred hereinafter as: A - raster data analysis and B - raw data analysis.

In strategy A the slice height of 0.5 m was based on the expert knowledge on olive orchard structure which allowed the filtering out of points reflected from ground and from low vegetation. The slice height of 0.5 m should not be mistaken for the optimal slice height for determining the tree center, as these strategies were totally independent from each other. In strategy B a radius of each buffer zone was defined as a half of the distance to the nearest tree centre. The minimum bounding polygons were created in each buffer zone using only LiDAR points with the height above 0.5 m. The polygons from the CHM slicing in strategy A and the minimum bounding polygons in strategy B can be considered as crown shapes. In this way, for each tree in total, four different crown shapes were created, i.e., using two strategies for the both sparse and dense LiDAR datasets. The area of each polygon was then calculated and the areas obtained using different strategies were mutually compared.

After obtaining the crown shape areas, it was checked whether the sample density has any influence on the crown area determination. The following samples were compared against each other:

1. Area residuals between the density of 9.0 points m^{-2} against the density of 3.5 points m^{-2}
2. Area values between the density of 0.5 points m^{-2} against the density of 3.5 points m^{-2} ;

3. Area values between the density of 0.5 points m^{-2} against the density of 9.0 points m^{-2} ;
4. Area values between the density of 0.5 points m^{-2} against the density of 3.5 or of 9.0 points m^{-2} .

Comparison 1 was made in the residual domain, because the samples contained different trees. Compared samples referred to the same trees for the comparisons 2, 3 and 4, thus, the value domain was used. The Kolmogorov-Smirnov test was performed to check whether the samples had a normal distribution before the comparison. For samples having a normal distribution, Levene's test was performed to check the homogeneity of variances. When both of the compared samples had a normal distribution, a paired sample *t*-test was performed: Student's *t*-test when variances of both samples were equal or Welch's *t*-test otherwise. If at least one of the compared samples did not have a normal distribution, a Mann-Whitney U test was performed. All the mentioned tests were performed at the significance level of $\alpha=0.05$.

It was also investigated whether the both strategies provided significantly different results. The same aforementioned statistical approach was used. However, this time, one sample contained data from strategy A (based on raster data) and the second sample from strategy B (based on raw data). These comparisons were made separately for each dataset with a different density, but always in the value domain.

Tree height, crown base height and average crown diameter

For each tree, the crown metrics were calculated using the FUSION software for LiDAR point clouds. Different minimum height filter values were used starting with 0.5 m, 1.0 m, 1.5 m and finishing with 2.0 m. The different filter heights always provided the same tree height; assumed as the height of the highest point in each dataset. This was not the case for the crown base height, because too large a filter value may have removed points belonging to the crown. The height of the crown base was taken from the metrics with minimum height filter set to 0.5 m, because for this setting the differences between crown heights and the value of the minimum height filter assumed the largest value. This can be explained in a way that 0.5 m of the height filter was entirely sufficient to remove ground points and low vegetation.

Finally, the obtained polygons of crown shapes were used to estimate the average crown diameter. For each polygon, an azimuthal grid of lines crossing the centroid of the polygon was imposed. The azimuths of the lines were in a range from 0 to 170 degrees, with a step of 10 degrees. The grid was clipped by the crown shape polygon and the length of each grid segment was measured. The length of the longest segment was assumed to be equal to the maximum diameter of a tree. The length of the perpendicular segment to the longest segment was assumed to be equal to the minimum diameter. The average crown diameter was calculated as a mean value of the both determined diameters, which is consistent with the methodology applied to the field measurements.

Statistical tests were performed to check whether the density of the dataset had any impact on the results and whether both strategies provided similar results. Exactly the same approach as for crown shape areas was used for other parameters however, the tests were performed separately for tree height, crown base height and average crown diameter.

LiDAR point distribution inside the crown

A standardisation of point heights was calculated, according to the following equation:

$$h^t = \frac{(H^t - H_{cb}^t)}{(H_{ct}^t - H_{cb}^t)} \quad [1]$$

where:

h^t - is the normalised height of LiDAR point, from 0 to 100 [%];

H^t - is the height of a LiDAR point above the DTM;

H_{ct}^t - is the height of a tree above the terrain obtained by field measurements;

H_{cb}^t - is the height of a crown base above the terrain obtained by field measurements.

In this way, the subsets of LiDAR points for all trees could be aggregated (separately for different LiDAR densities) and presented as a model of point distribution inside the crown. Moreover, a histogram representing the amount of points at different levels of tree crown was created. The Kolmogorov-Smirnov test were performed on normalised heights in order to check if the reflected LiDAR points inside the tree crown had a normal distribution.

Relationship between tree size and quality of the results

The relationship between the tree size and the accuracy of determined tree parameters, i.e., tree height, crown base height, average crown diameter, and the crown shape area, was examined in order to investigate whether the accuracy of proposed strategies depends on the tree size. The accuracy was assessed as a difference between the estimated value and the value obtained from the field measurements. Trees were divided into two groups on a basis of the tree stem diameter. The Mann-Whitney U test was performed using the significance level of $\alpha=0.05$, because the number of trees per each group was different. A null hypothesis was that the quality of the results was the same for trees of different size.

Moreover, a linear regression between the stem diameter and the accuracy of each parameter was determined and the regression coefficients were compared using the Mann-Whitney U test in order to fully benefit from the quantitative character of the tree size indicator. The linear regression allowed the verification as to whether the accuracy is better or worse for large trees. Figures showing the relationship between the tree size indicator and the accuracy of obtained parameters were also prepared.

In total, 16 tests were performed: for every possible combination of four tree parameters, for two LiDAR datasets, and for two strategies.

Results and discussion

Digital Terrain Model, Canopy Height Model and crown centers

The best quality for both of the datasets came from DTM models based on averaging heights inside each cell. Subsequently, a 5x5 m model for the sparse LiDAR dataset and a 4x4 m model for the dense LiDAR dataset were used. For both models, the standard

deviation of residuals with respect to GPS heights was equal to 13 cm, whereas the mean bias was below 1 cm.

The point clouds were normalised using the chosen DTMs (see Fig. 2). In both datasets about 5% of the points had negative heights above the ground (up to -0.26 m), which indicated that the quality of generated DTMs was rather poor for some areas. The points with negative relative heights were located on scarps close to terraces, which separate the ground levels in the orchard. The selected trees were located far from these scarps, and thus, the normalised point clouds could be used in subsequent analyses.

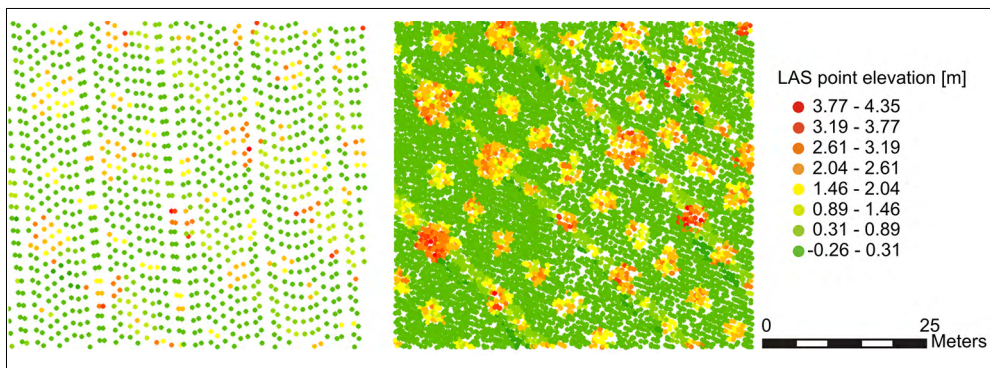


Figure 2 - Normalised point cloud for sparse (left) and dense (right) dataset for the same area.

The polygons from CHM slicing were assessed visually. For heights below 0.3 m some trees were connected and thus represented by a single polygon, whereas for heights higher than 2.0 m some trees were represented by more than one polygon. Therefore, the standard deviation of a distance between the location of a reference tree and the automatically determined tree center was calculated only for slice heights between 0.3 m and 2.0 m (Fig. 3). For the sparse point cloud, the centroid accuracy changed along with the height of the CHM slice. For low-height slices the standard deviation reached up to 2.3 m and for high-height slices the standard deviation reached up to 1.7 m. The smallest distances between the reference trees and the automatically derived tree centers were obtained for slice heights from 0.8 to 1.2 m with a standard deviation below 0.3 m. The minimum standard deviation of 0.24 m was obtained for the slice height of 1.0 m. For the dense LiDAR data, the accuracy of centroids was similar for every slice height with a standard deviation below 0.3 m. For the height slices between 0.9 m and 1.1 m the distances were smallest with a standard deviation of 0.24 m. We can thus conclude that the height of 1.0 m for CHM slicing provides the most accurate and the most reliable location of tree centroid for both sparse and dense LiDAR datasets.

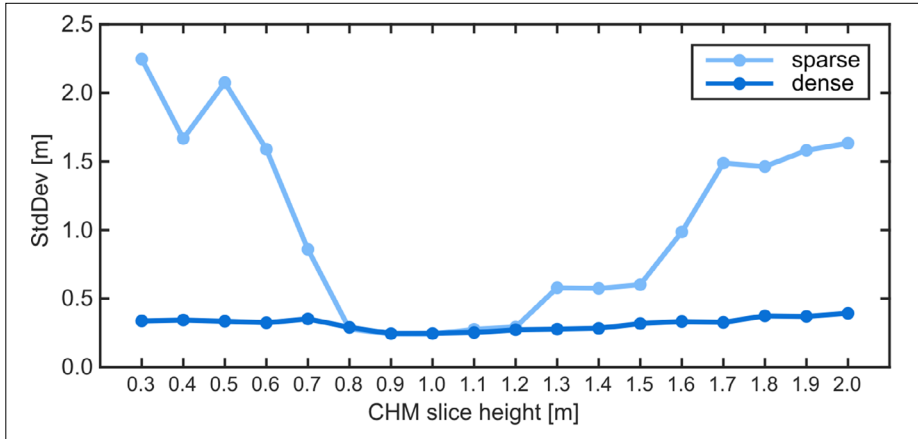


Figure 3 - Standard deviation of centroid distances from reference tree centers for different CHM slice heights.

Crown shape and area

Following the two proposed strategies, the polygons representing crown shape were obtained from raster and raw data and for the point clouds of different densities. Crown shapes were illustrated together with LiDAR points inside the polygons in Figure 4 for four selected representative trees in order to compare the shapes obtained with different strategies and datasets. For the majority of trees the crown contours obtained using different strategies were similar to each other (e.g., tree no. 6). The dense LiDAR dataset allowed more consistent crown shapes to be determined than the sparse dataset (i.e., between the strategies based on the raster and raw data analysis.) For some trees, reliable tree crowns were not obtained using strategy B and the sparse dataset, because of the insufficient number of detected points (e.g., for trees no. 10 and 15). Usually, the area of a crown is larger for CHM sliced polygons than for minimum bounding polygons, because the strategy A with CHM sliced polygons takes into account the entire cell surrounding each point.

Figure 5 shows areas of tree crowns estimated using different strategies and different LiDAR datasets. The areas determined using dense LiDAR dataset in both strategies were close to each other with a standard deviation of 1.7 m². However, there was a clear systematic error between the solutions: the mean difference between strategy A and strategy B was -3.9 m². The areas determined with the CHM raster slicing were larger than when using the minimum bounding polygon method. It is impossible to assess reliably which strategy is more precise, as no field measurements were made to determine the true tree crown areas. The strategy B failed also for the sparse data analysis, because the areas were remarkably underestimated compared with the other solutions. For the sparse dataset, much better results were obtained from the raster analysis. A small bias of 0.5 m² was found when comparing the results from strategy A for the sparse and dense datasets. However, the standard deviation thereof was relatively large, i.e., 5.2 m².

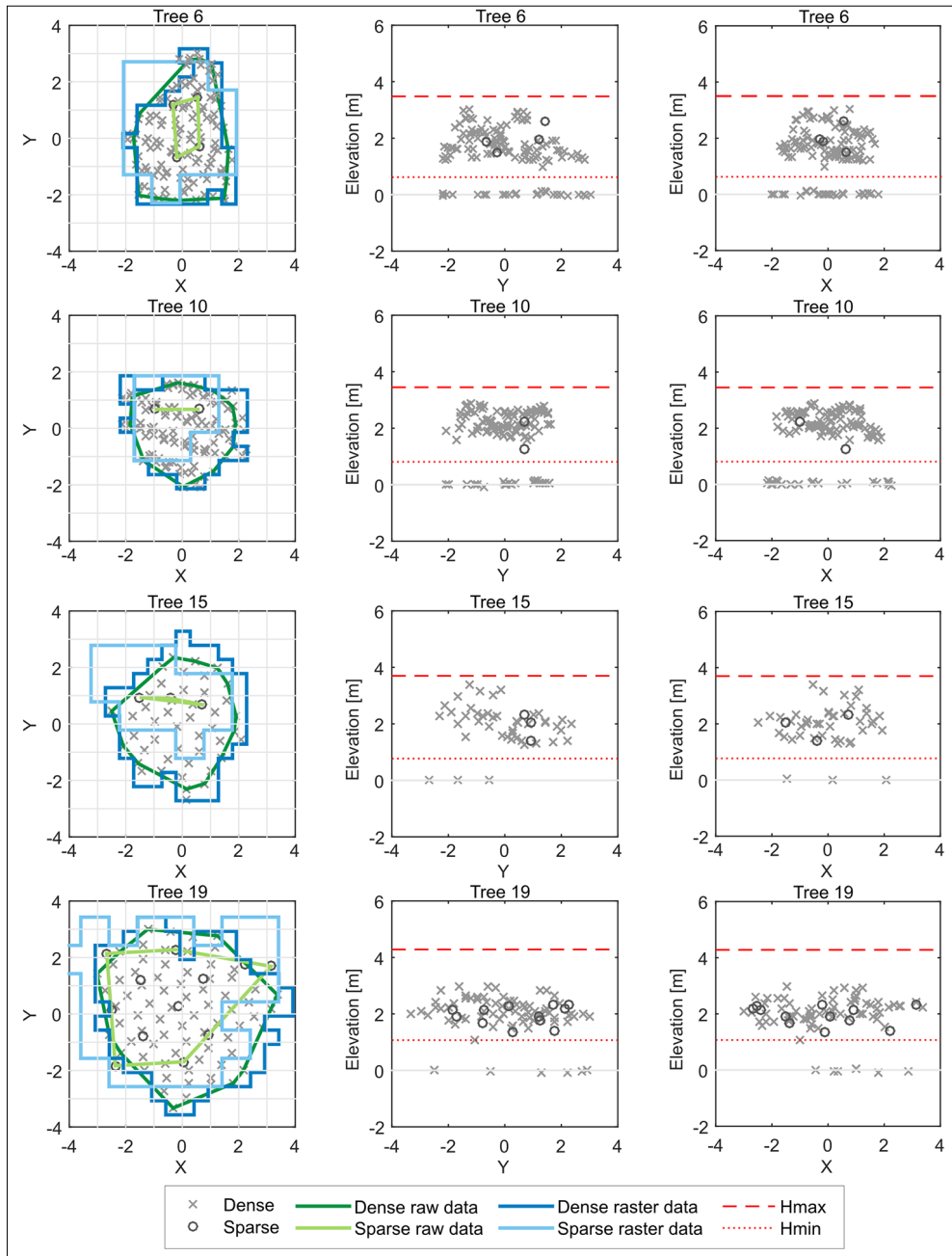


Figure 4 - Projections of LiDAR points (grey circles for sparse dataset and grey crosses for dense dataset) within the area of a tree; crown shapes from various methods are presented on top view (left column); X=0 and Y=0 coordinates represent the location of a reference tree center.

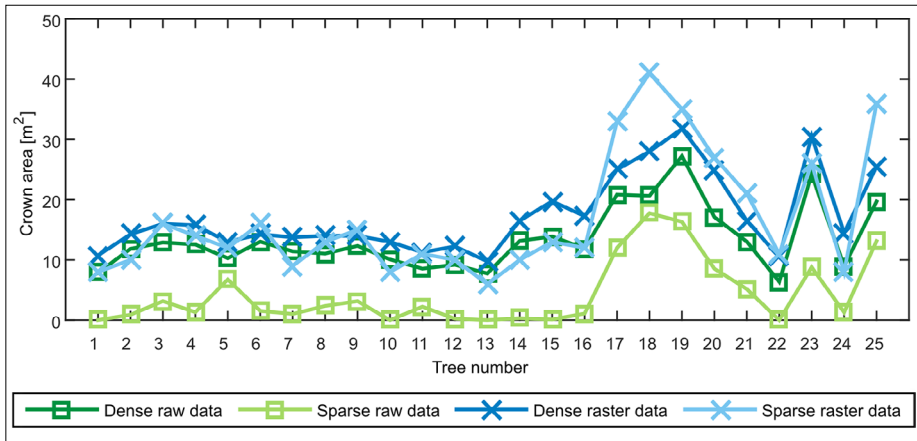


Figure 5 - Estimated tree crown areas.

It was impossible to assess whether the results obtained for the area of overlaying scans were different than those for the remaining area, because of the lack of crown area measurements. The Mann-Whitney U test in value domain (Tab. 2) confirmed, however, that the results were not similar among the sparse and dense datasets, but only for the raw data analysis. In contrast, the test accepted the hypothesis about the similarity of the samples for raster data analysis. In other words, the estimated crown areas did not depend on the dataset density for strategy A.

Table 2 - The p-values of Mann-Whitney U test (* t-test) for the similarity of results between datasets of different density

Density of sample 1 [point m ⁻²]	Density of sample 2 [point m ⁻²]	Number of trees	p-value for raster data	p-value for raw data
0.5	3.5	12	0.862	0.002*
0.5	9	13	0.143	0.000*
0.5	3.5 and 9.0	25	0.177	0.000

Further statistical analyses indicated that both strategies are not equivalent for the estimation of the crown shape area. For the sparse dataset, Mann-Whitney U test returned p=0.000, whereas paired sampled t-test returned p=0.002 for the point density of 9.0 m⁻², and p=0.050 for the point density of 3.5 m⁻². Mann-Whitney U test for the entire dense dataset returned p=0.008.

Tree height, crown base height and average crown diameter

The values of tree heights, crown base heights and average crown diameters obtained from the field measurements and from the analysis of LiDAR data are shown separately for each tree in Figure 6. The statistics of differences between estimated and measured values are shown in Figure 7 in a form of box-plots depicting the quartiles, three-sigma range, and outliers.

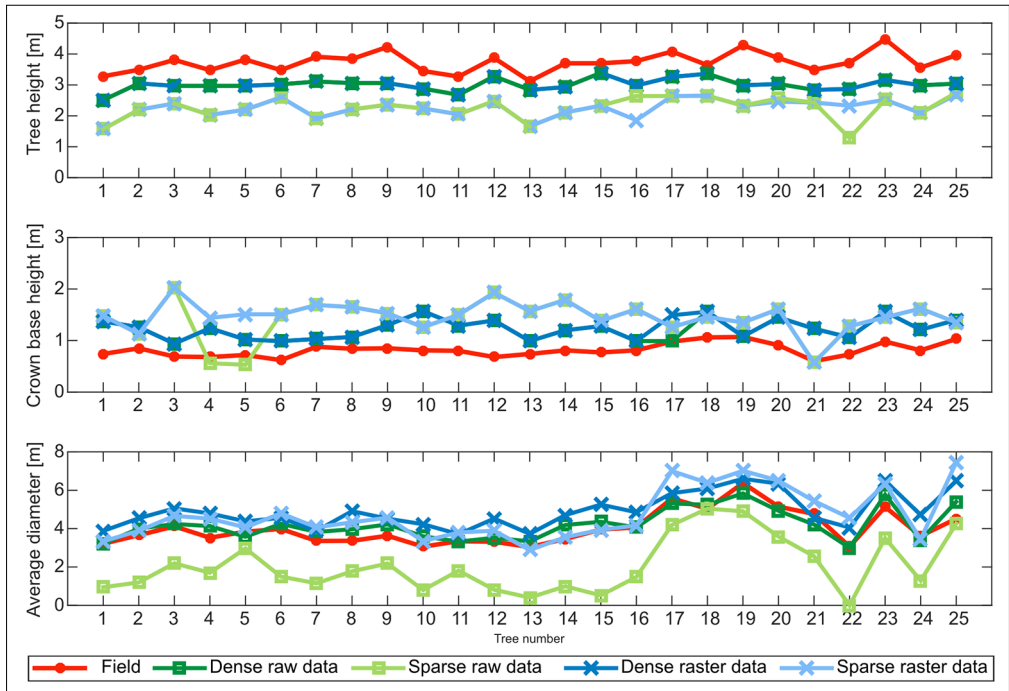


Figure 6 - Values of tree height, crown base height and average crown diameter obtained from field measurements and estimated from LiDAR data.

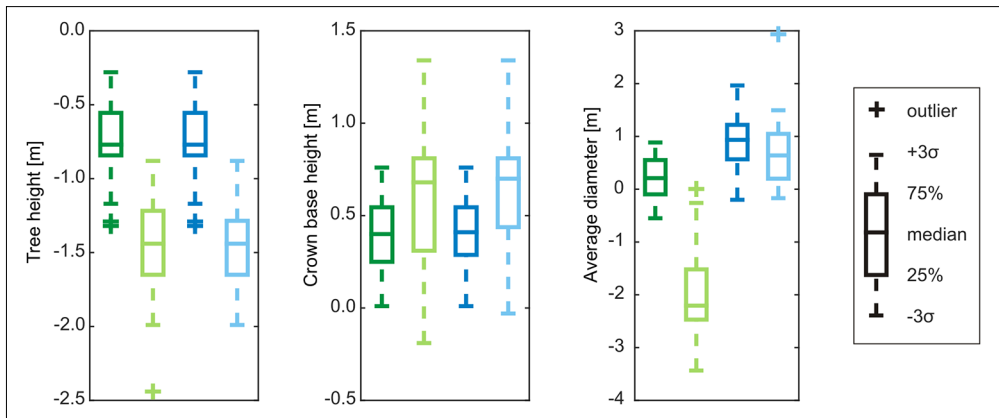


Figure 7 - Box-plots of differences between the estimates and field measurements for: tree heights, crown base heights and average crown diameters.

Tree heights were underestimated with respect to the field measurements and the errors were larger for the sparse dataset with a bias of -1.48 m, when compared with the dense dataset with a bias of -0.72 m. Strategy A and B provided almost the same results of the tree heights: in the dense dataset there were no differences at all, whereas for the sparse

dataset only three estimated tree heights were different. The standard deviation of residuals with respect to field measurements was equal to 0.28 m for the both strategies when using the dense dataset, 0.36 m and 0.30 for strategy A and B, respectively when using the sparse dataset.

Crown base heights were usually overestimated and the errors were large for the sparse dataset with a bias of +0.66 and +0.59 m for strategy A and B, respectively. For the dense dataset the errors were smaller with a bias of +0.42 m and +0.40 m for strategy A and B, respectively. Therefore, both strategies again returned very similar results.

The estimated length of the average crown diameter varies between the strategies and datasets. The values obtained with strategy B and the sparse dataset were always underestimated and clearly outlying (with a bias of -1.94 m and a standard deviation of 0.79 m), which can be related to the poor results of the estimation of the crown areas. In contrast, strategy B provided the most accurate results for the dense dataset, equalling to $+0.19 \text{ m} \pm 0.40 \text{ m}$. Strategy A provided a closer similarity between the results for the both datasets. Biases of +0.90 and +0.71 m were obtained for the dense and sparse point clouds, respectively, with the standard deviations of 0.47 and 0.69 m.

For the both raster and raw data analysis there were no significant differences for the field measurements in the residual domain between the results obtained using the datasets of densities of 9.0 and 3.5 points m^{-2} according to a paired sample *t*-test (Tab. 3). However, a paired sample *t*-test for the similarity of the results obtained using the sparse and dense dataset (Tab. 4) showed that the values of estimated tree heights, crown base heights, and average crown diameters were different, except for the average crown diameter in strategy A. This exception corresponds to the result obtained for the determination of the crown shape areas, whose values did not depend on the density of dataset in the raster analysis.

Table 3 - The p-values of paired sample *t*-test for the similarity between the results obtained for datasets of 9.0 points m^{-2} and 3.5 points m^{-2} density (residual domain).

Tree parameter	Raster data	Raw data
Tree height	0.295	0.295
Crown base height	0.840	0.486
Average crown diameter	0.695	0.220

Table 4 - The p-values of paired sample *t*-test for the similarity of results between the dense and sparse datasets (in the value domain).

Tree parameter	Raster data	Raw data
Tree height	0.000	0.000
Crown base height	0.000	0.003
Average crown diameter	0.240	0.000

Further statistical analyses shown in Table 5 indicated that both strategies are equivalent for the estimation of tree heights and crown base heights, but not for average crown diameter. This again corresponds to the results obtained for crown shape area.

Table 5 - The p-values of Mann-Whitney U test (* or paired sample *t*-test) for the equivalence of strategies.

Dataset density [points m ⁻²]	Number of trees	Tree height	Crown base height	Average crown diameter
9.0	13	1.000	1.000	0.002
3.5	12	1.000	0.617	0.031
9.0 and 3.5	25	1.000	0.723	0.004*
0.5	25	0.966	0.662*	0.000*

LiDAR point distribution inside the crown

Figure 8 shows a normalised LiDAR point distribution inside the crown for each dataset density. For both densities of point clouds, points were typically concentrated in the central part of a crown. Side views show that for the sparse point cloud all points were located below the level of 70% of the crown height and for the dense point cloud below the level of 90%. This indicates that no points were detected at the ends of top branches. For the sparse point cloud, some points located below the measured crown base, i.e., by the means of the negative normalised height, were poorly identified because of a poor DTM quality in some areas. The Kolmogorov-Smirnov test rejected the hypothesis about the normal distribution of data. For the dense dataset, 70% of points were located between 30% and 60% of the crown height, and for the sparse dataset between 25% and 50%, which was probably related to a higher tree density, i.e., thicker branches and more leaves, in central and central-bottom parts of a tree.

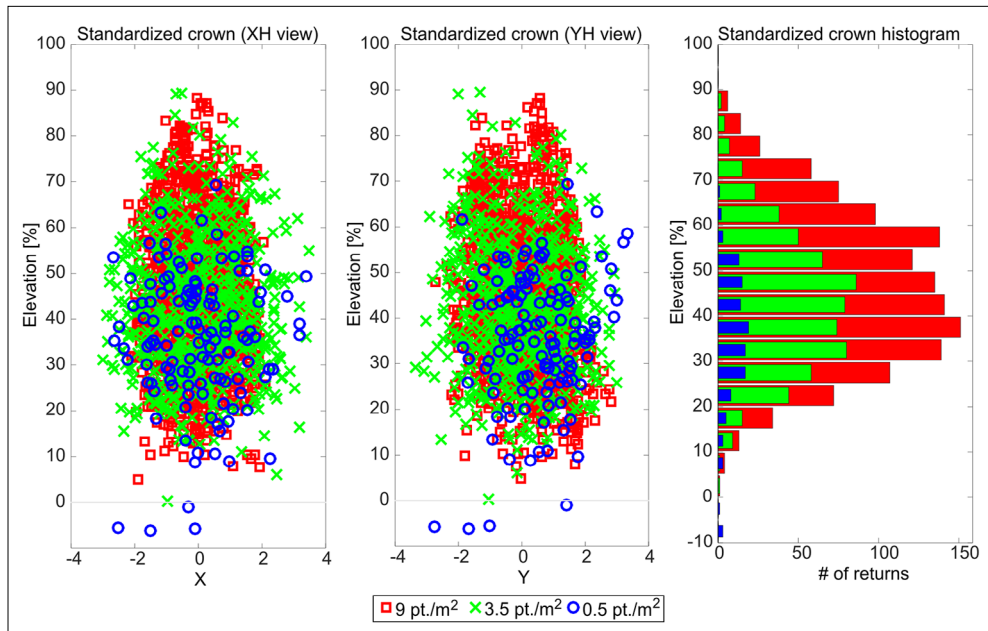


Figure 8 - LiDAR data point distribution in standardised tree crown in side views (left and center) and histogram of point distribution (right) for the dense (overlapping scans - red, other - green) and the sparse (blue) LiDAR datasets.

Impact of the tree size on the accuracy of results

Trees were divided into two groups on a basis of a stem diameter. By that means, the group of medium trees contained 17 trees, whereas the group of large trees contained 8 trees. All trees located in the area of overlaying scans were included in the group of medium trees, which was the disadvantage of this division.

The Mann-Whitney U test accepted the null hypothesis ($p > 0.05$) only in three cases for the sparse dataset analysis (Tab. 6). In both strategies the accuracy of the crown base height depended on the tree size ($p = 0.005$ and $p = 0.044$ for strategy A and B, respectively). For strategy A the aforementioned dependency was confirmed by the determination coefficients $R^2 = 0.35$, and the linear regression model indicating that for larger trees the crown base heights were more accurate. A significant dependency ($p = 0.023$) was also noted for the relationship between the tree size and the accuracy of the average crown diameter for the sparse dataset analysis when using strategy A. However, this was not confirmed by the determination coefficient which assumes the value of $R^2 = 0.18$. Otherwise, the accuracy of estimated parameters appeared to be independent from the size of a tree.

Table 6 - The p-values of Mann-Whitney U test and determinations coefficients R^2 for the relation between the stem diameter and the accuracy of the estimated tree parameter.

Parameter	Dataset	Raster data		Raw data	
		p-value	R^2	p-value	R^2
Tree height	dense	0.080	0.13	0.080	0.13
	sparse	0.977	0.00	0.190	0.03
Crown base height	dense	0.748	0.00	0.683	0.10
	sparse	0.005	0.35	0.044	0.11
Average crown diameter	dense	0.683	0.07	0.190	0.15
	sparse	0.023	0.18	0.290	0.19

Summary and conclusions

In order to analyse how LiDAR data density impacts on the accuracy of automatically estimated geometric parameters of olive trees such as tree height, crown base height, average crown diameter and crown shape area, two processing strategies were proposed and verified: one based on the raster analysis, and the second on raw LiDAR data. When possible, the estimated parameters were compared with field measurements. The similarity of the results obtained from datasets of different densities was subject to statistical tests. In particular, the dependency of tree size on the accuracy of estimated parameters was investigated.

As expected, the parameters estimated from the dense LiDAR data were more accurate than those obtained from the sparse LiDAR data analysis. The difference of the accuracy was especially remarkable for the estimation of tree heights and crown base heights. Since the distribution of a mass in the crown is uneven, the majority of LiDAR pulses were reflected from the central part of a crown, and it was unlikely to obtain any reflections from top or bottom branches when using a low scanning density. For tree heights and crown base heights, the choice of the estimation strategy was irrelevant, as the both strategies returned the same or very similar results.

The choice of a strategy was fundamental for the crown shape area and for the average

crown diameter. When processing the dense dataset, the raw data analysis provided the most accurate results. The results from the raster analysis were slightly biased, i.e., the average crown diameters were overestimated and slightly less accurate. However, the raw data analysis resulted in a very poor determination of the crown shape area and the average crown diameters. This effect was overcome with the raster data analysis, wherein the results from the sparse and dense dataset do not differ statistically. This is an important finding, showing that the LiDAR data of low density may be useful for some agricultural management purposes.

Finally, it was shown that the accuracy of estimated tree parameters is generally independent of the tree size. The only exception was found for crown base heights obtained from the sparse dataset, where the results were slightly more accurate for large trees, however, the accuracy of these results was very poor anyway.

Acknowledgements

The authors appreciate the financial support provided by the Vice-Rectorate for Research of the Universitat Politècnica de València [Grant PAID-06-12-3297; SP20120534].

References

- Andersen H.E., Reutebuch S.E., McGaughey R.J. (2006) - *A rigorous assessment of tree height measurements obtained using airborne lidar and conventional field methods*. Canadian Journal of Remote Sensing, 32 (5): 355-366. doi: <http://dx.doi.org/10.5589/m06-030>.
- Araújo M., Higuchi N., Carvalho J. (1999) - *Comparison of formula for biomass content determination in a tropical rain forest site in the state of Pará, Brazil*. Forest Ecology and Management, 117: 43-52. doi: [http://dx.doi.org/10.1016/s0378-1127\(98\)00470-8](http://dx.doi.org/10.1016/s0378-1127(98)00470-8).
- Brandtberg T. (1999) - *Automatic individual tree-based analysis of high spatial resolution remotely sensed data*. Doctoral thesis. Acta Universitatis Agriculturae Sueciae, Silvestria 118. Swedish University of Agricultural Sciences, Centre for Image Analysis. Uppsala, Sweden.
- Brunner A. (1998) - *A light model for spatially explicit forest stands models*. Forest Ecology and Management, 147: 19-46. doi: [http://dx.doi.org/10.1016/s0378-1127\(97\)00325-3](http://dx.doi.org/10.1016/s0378-1127(97)00325-3).
- Doruska P., Burkhart H. (1994) - *Modeling the diameter and locational distribution of branches within the crowns of loblolly pine trees in unthinned plantations*. Canadian Journal of Forest Research, 24: 2362-2376. doi: <http://dx.doi.org/10.1139/x94-305>.
- Edson C., Wing M.G. (2011) - *Airborne Light Detection and Ranging (LiDAR) for individual tree stem location, height, and biomass measurements*. Remote Sensing, 3: 2494-2528. doi: <http://dx.doi.org/10.3390/rs3112494>.
- Estornell J., Velázquez-Martí B., López-Cortés I., Salazar D., Fernández-Sarría A. (2014) - *Estimation of wood volume and height of olive tree plantations using airborne discrete-return LiDAR data*. GIScience & Remote Sensing, 51 (1): 17-29. doi: <http://dx.doi.org/10.1080/15481603.2014.883209>.
- Evans J.S., Hudak A.T., Faux R., Smith A.M.S. (2009) - *Discrete return LiDAR in natural resources: Recommendations for project planning, data processing, and deliverables*. Remote Sensing, 1: 776-794. doi: <http://dx.doi.org/10.3390/rs1040776>.
- Francis J. (2000) - *Estimating biomass and carbon content of saplings in Puerto Rican*

- secondary forests*. Caribbean Journal of Science, 36: 346-350.
- Hauglin M., Dibdiakova J., Gobakken T., Næsset E. (2013) - *Estimating single-tree branch biomass of Norway spruce by airborne laser scanning*. ISPRS Journal of Photogrammetry and Remote Sensing, 79: 147-156. doi: <http://dx.doi.org/10.1016/j.isprsjprs.2013.02.013>.
- Hinsley S., Hill R., Gaveau D., Bellamy P. (2002) - *Quantifying woodland structure and habitat quality for birds using airborne laser scanning*. Functional Ecology, 16 (6): 851-857. doi: <http://dx.doi.org/10.1046/j.1365-2435.2002.00697.x>.
- Holmgren J., Persson Å. (2003) - *Identifying species of individual trees using airborne laser scanning*. Remote Sensing of Environment, 90 (4): 415-423. doi: [http://dx.doi.org/10.1016/S0034-4257\(03\)00140-8](http://dx.doi.org/10.1016/S0034-4257(03)00140-8).
- Hopkinson C., Chasmer L., Young-Pow C., Treitz P. (2004) - *Assessing forest metrics with a ground-based scanning lidar*. Canadian Journal of Forest Research, 34 (3): 573-583. doi: <http://dx.doi.org/10.1139/x03-225>.
- Houghton R.A., Hall F., Goetz S.J. (2009) - *Importance of biomass in the global carbon cycle*. Journal of Geophysical Research, 114: 1-13. doi: <http://dx.doi.org/10.1029/2009jg000935>.
- Hyypä J., Inkinen M. (1999) - *Detecting and estimating attributes for single trees using laser scanner*. The Photogrammetric Journal of Finland, 16: 27-42.
- Kankare V., Rätty M., Yu X., Holopainen M., Vastaranta M., Kantola T., Hyypä J., Hyypä H., Alho P., Viitala R. (2013) - *Single tree biomass modelling using airborne laser scanning*. ISPRS Journal of Photogrammetry and Remote Sensing, 85: 66-73. doi: <http://dx.doi.org/10.1016/j.isprsjprs.2013.08.008>.
- Lefsky M.A., Cohen W.B., Parker G.G., Harding D.J. (2002) - *LiDAR remote sensing for ecosystem Studies*. BioScience, 52: 19-30. doi: [http://dx.doi.org/10.1641/0006-3568\(2002\)052\[0019:lrsfes\]2.0.co;2](http://dx.doi.org/10.1641/0006-3568(2002)052[0019:lrsfes]2.0.co;2).
- Magnussen S., Eggermonth P., La Riccia V. (1999) - *Recovering tree heights from airborne laser scanner data*. Forest Science, 45: 407-422.
- Means J., Acker S., Fitt B., Renslow M., Emerson L., Hendrix C. (2000) - *Predicting forest stand characteristics with airborne scanning lidar*. Photogrammetric Engineering and Remote Sensing, 66 (11): 1367-1371.
- Morsdorf F., Meier E., Kötz B., Itten K., Dobbertin M., Allgöwer B. (2004) - *Lidar-based geometric reconstruction of boreal type forest stands at single tree level for forest and wildland fire management*. Remote Sensing of Environment, 92 (3): 353-362. doi: <http://dx.doi.org/10.1016/j.rse.2004.05.013>.
- Persson A., Holmgren J., Söderman U. (2002) - *Detecting and measuring individual trees using an airborne laser scanner*. Photogrammetric Engineering & Remote Sensing, 68: 925-932.
- Pope G., Treitz P. (2013) - *Leaf Area Index (LAI) estimation in boreal mixedwood forest of Ontario, Canada using Light Detection and Ranging (LiDAR) and WorldView-2 imagery*. Remote Sensing, 5: 5040-5063. doi: <http://dx.doi.org/10.3390/rs5105040>.
- Popescu S.C. (2007) - *Estimating biomass of individual pine trees using airborne lidar*. Biomass and Bioenergy, 31 (9): 646-655. doi: <http://dx.doi.org/10.1016/j.biombioe.2007.06.022>.
- Popescu S.C., Zhao K. (2008) - *A voxel-based lidar method for estimating crown base*

- height for deciduous and pine trees*. Remote Sensing of Environment, 112 (3): 767-781. doi: <http://dx.doi.org/10.1016/j.rse.2007.06.011>.
- Ramdani F. (2013) - *Urban vegetation mapping from fused hyperspectral image and LiDAR data with application to monitor urban tree heights*. Journal of Geographical Systems, 5 (4): 404-408. doi: <http://dx.doi.org/10.4236/jgis.2013.54038>.
- Reutebuch S.E., Andersen H.E., McGaughey R.J. (2005) - *Light Detection and Ranging (LiDAR): An Emerging Tool for Multiple Resource Inventory*. Journal of Forestry, 103 (6): 286-292.
- Riaño D., Valladares F., Condés S., Chuvieco E. (2004) - *Estimation of leaf area index and covered ground from airborne laser scanner (lidar) in two contrasting forests*. Agricultural and Forest Meteorology, 124 (3-4): 269-275. doi: <http://dx.doi.org/10.1016/j.agrformet.2004.02.005>.
- Roberts S.D., Dean T.J., Evans D.L., McCombs J.W., Harrington R.L., Glass P.A. (2005) - *Estimating individual tree leaf area in loblolly pine plantations using LiDAR-derived measurements of height and crown dimensions*. Forest Ecology and Management, 213 (1-3): 54-70. doi: <http://dx.doi.org/10.1016/j.foreco.2005.03.025>.
- Rodríguez R., Valencia S., Meza J., Capó M., Reynoso A. (2008) - *Crecimiento y características de la copa de procedencias de Pinus gregii Engelm.* Fitotecnia, 31 (1): 19-26.
- Sabol J., Patočka Z., Mikita T. (2014) - *Usage of LiDAR data for leaf area index estimation*. GeoScience Engineering, 60 (3): 10-18. doi: <http://dx.doi.org/10.2478/gse-2014-0013>.
- Saremi H., Kumar L., Stone C., Melville G., Turner R. (2014) - *Sub-compartment variation in tree height, stem diameter and stocking in a Pinus radiata D. Don Plantation examined using airborne LiDAR data*. Remote Sensing, 6 (8): 7592-7609. doi: <http://dx.doi.org/10.3390/rs6087592>.
- Sheridan R.D., Popescu S.C., Gatzolis D., Morgan C.L.S., Ku N-W. (2015) - *Modeling Forest Aboveground Biomass and Volume Using Airborne LiDAR Metrics and Forest Inventory and Analysis Data in the Pacific Northwest*. Remote Sensing, 7 (1): 229-255. doi: <http://dx.doi.org/10.3390/rs70100229>.
- St-Onge B., Treitz P., Wulder M. (2003) - *Tree and canopy height estimation with scanning Lidar*. Remote Sensing of Forest Environments, 489-510. doi: http://dx.doi.org/10.1007/978-1-4615-0306-4_19.
- Straub C., Koch B. (2011) - *Estimating single tree stem volume of Pinus sylvestris using airborne laser scanner and multispectral line scanner data*. Remote Sensing, 3 (12): 929-944. doi: <http://dx.doi.org/10.3390/rs3050929>.
- Tomppo E. (1997) - *Recent status and further development of Finnish multisource forest inventory*. Proceedings of The Marcus Wallenberg Foundation Symposia, 11: 53-70.
- Vauhkonen J. (2010) - *Estimating crown base height for Scots pine by means of the 3D geometry of airborne laser scanning data*. International Journal of Remote Sensing, 31 (5): 1213-1226. doi: <http://dx.doi.org/10.1080/01431160903380615>.
- Velázquez-Martí B., Fernández-González E., Estornell J., Ruiz L.A. (2010) - *Dendrometric and dasometric analysis of the bushy biomass in Mediterranean forests*. Forest Ecology and Management, 259: 875-882. doi: <http://dx.doi.org/10.1016/j.foreco.2009.11.027>.
- Velázquez-Martí B., López Cortés I., Salazar-Hernández D.M. (2014) - *Dendrometric analysis of olive trees for wood biomass quantification in Mediterranean orchards*.

Agroforestry Systems, 88 (5): 755-765. doi: <http://dx.doi.org/10.1007/s10457-014-9718-1>.

Yu X., Hyypä J., Kaartinen H., Maltamo M. (2004) - *Automatic detection of harvested trees and determination of forest growth using airborne laser scanning*. Remote Sensing of Environment, 90 (4): 451-462. doi: <http://dx.doi.org/10.1016/j.rse.2004.02.001>.

© 2016 by the authors; licensee Italian Society of Remote Sensing (AIT). This article is an open access article distributed under the terms and conditions of the Creative Commons Attribution license (<http://creativecommons.org/licenses/by/4.0/>).